Comparative study of InGaP/GaAs high electron mobility transistors with upper and lower delta-doped supplied layers

© Jung-Hui Tsai[¶], Sheng-Shiun Ye, Der-Feng Guo[*], Wen-Shiung Lour[+]

Department of Electronic Engineering, National Kaohsiung Normal University,
116 Ho-ping 1st Road, Kaohsiung 824, Taiwan
[*] Department of Electronic Engineering, Air Force Academy, Kaohsiung,
Sisou 1, Jieshou W. Rd., Gangshan Dist., Kaohsiung City 820, Taiwan
[+] Department of Electrical Engineering, National Taiwan Ocean University,
2 Peining Road, Keelung 202, Taiwan

(Получена 1 сентября 2011 г. Принята к печати 23 сентября 2011 г.)

Influence corresponding to the position of δ-doped supplied layer on InGaP/GaAs high electron mobility transistors is comparatively studied by two-dimensional simulation analysis. The simulated results exhibit that the device with lower δ-doped supplied layer shows a higher gate potential barrier height, a higher saturation output current, a larger magnitude of negative threshold voltage, and broader gate voltage swing, as compared to the device with upper δ-doped supplied layer. Nevertheless, it has smaller transconductance and inferior high-frequency characteristics in the device with lower δ-doped supplied layer. Furthermore, a knee effect in current–voltage curves is observed at low drain–to–source voltage in the two devices, which is investigated in this article.

1. Introduction

High electron mobility transistors (HEMTs) have attracted significant interest for high–speed digital and microwave circuit applications because the carriers in channel only transport in two-dimension direction [1–3]. Previously, InGaP/GaAs material system has been employed in HEMTs, attributed to

(i) the low surface recombination velocity of InGaP layer,

(ii) the conduction band discontinuity ($\Delta E_C \approx 0.2$ eV) at $In_{0.49}Ga_{0.51}P$/GaAs interface acting as a high gate barrier to provide good confinement effect for electrons in channel and increase the gate forward voltage,

(iii) the absence of deep level trap for improving output current decay and threshold voltage shift,

(iv) the low oxygen reactivity of the InGaP material to improve the device reliability, and

(v) the high chemical etching selectivity between InGaP and GaAs layers [4–8].

Therefore, high uniformity and yield could be achieved in device fabrication process. Because the gate barrier layer is undoped and large energy gap, it has good Schottky characteristic to improve gate forward voltage and enhance drain current.

In order to increase gate breakdown voltage and reduce leakage current in HEMTs, the δ-doped supplied layer is generally placed below the undoped gate barrier layer [8,9]. A two–dimensional electron gas (2DEG) is formed and confined at heterojunction by a δ-doped supplied layer. Furthermore, the δ-doped supplied layer below undoped channel layer is another approach to form 2DEG in channel. Liu et al. had demonstrated an inverted (lower) δ-doped HEMT, which provides wide operation region in dc and microwave characteristics [9]. Though excellent performance of HEMTs with upper and lower δ-doped supplied layers has been achieved, the difference of both devices has not been depicted and compared. In this article, we first demonstrate the effect corresponding to the position of δ-doped supplied layer on InGaP/GaAs HEMTs. DC and high–frequency characteristics will be

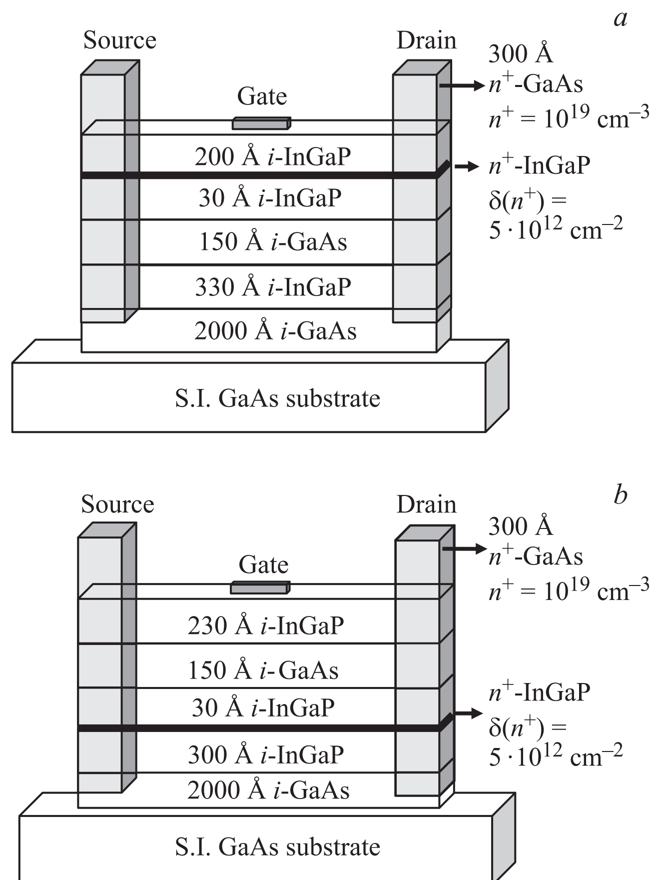

Figure 1. Schematic cross sectons of (*a*) device A with an upper δ-doped supplied layer and (*b*) device B with a lower δ-doped supplied layer.

[¶] E-mail: jhtsai@nknucc.nknu.edu.tw

analyzed and compared for the devices with upper and low δ-doped supplied layers.

2. Device structures

The studied devices were constructed on semi-insulating GaAs substrates. The layer structure of the $In_{0.49}Ga_{0.51}P$/GaAs HEMT with an upper δ-doped supplied layer, labeled device A, included a 2000 Å undoped GaAs buffer layer, a 330 Å undoped InGaP layer, a 150 Å undoped GaAs channel layer, a 30 Å undoped InGaP spacer layer, a $\delta(n^+) = 5 \cdot 10^{12}\,\text{cm}^{-2}$ δ-doped supplied layer, a 200 Å undoped InGaP gate layer, and a 300 Å $n^+ = 10^{19}\,\text{cm}^{-3}$ GaAs cap layer.

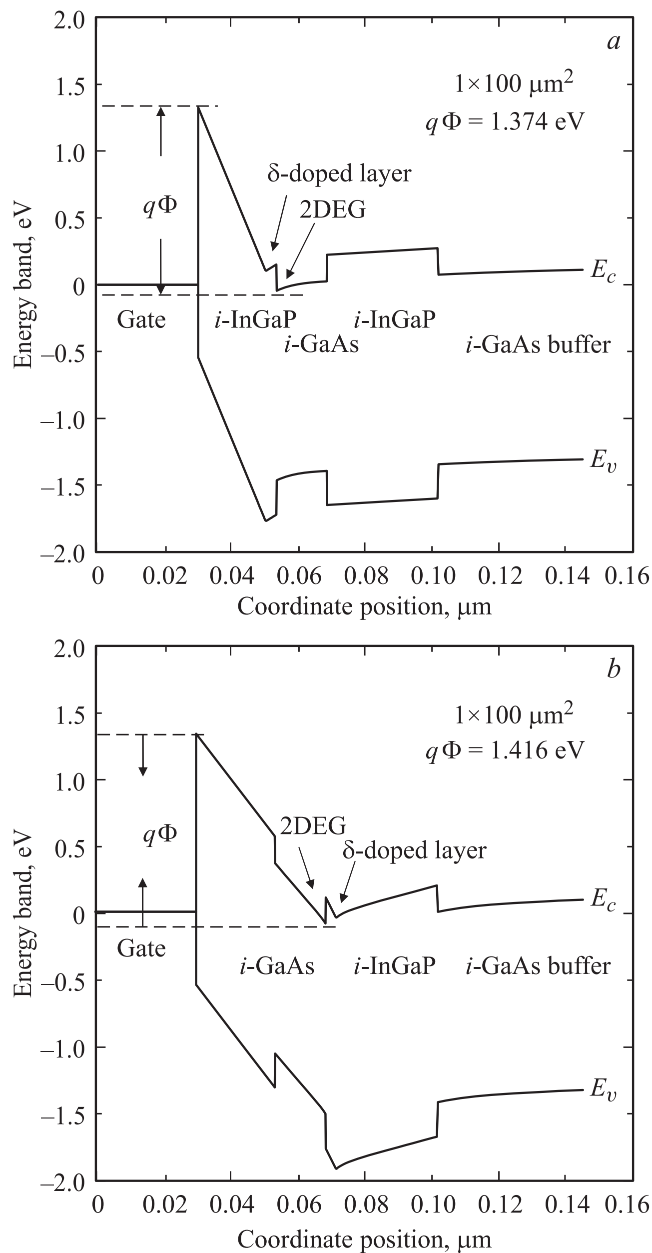

Figure 2. Energy-band diagrams at equilibrium of (a) device A and (b) device B.

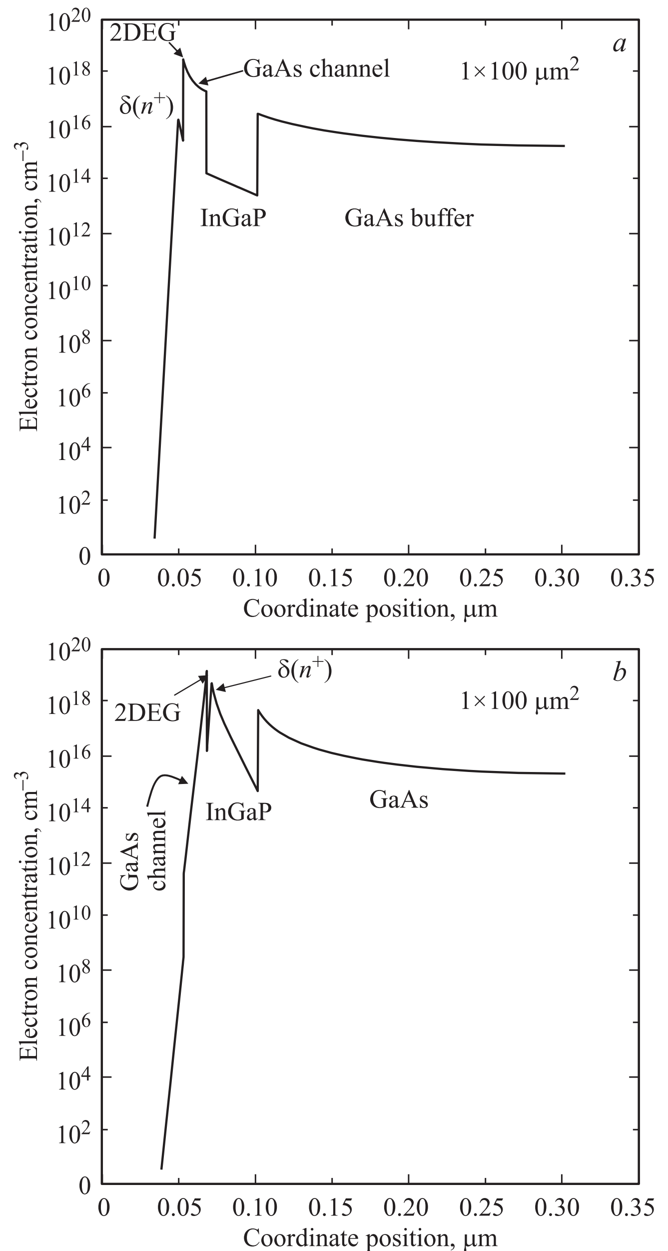

Figure 3. Electronic distributions at equilibrium of (a) device A and (b) device B.

Comparably, another $In_{0.49}Ga_{0.51}P$/GaAs HEMT with a lower δ-doped supplied layer, labeled device B, consisted of a 2000 Å undoped GaAs buffer layer, a 300 Å undoped InGaP layer, a $\delta(n^+) = 5 \cdot 10^{12}\,\text{cm}^{-2}$ δ-doped supplied layer, a 30 Å undoped InGaP spacer layer, a 150 Å undoped GaAs channel layer, a 230 Å undoped InGaP Schottky layer, and a 300 Å $n^+ = 10^{19}\,\text{cm}^{-3}$ GaAs cap layer.

In the two devices, the concentrations of δ-doped supplied layers and the total thickness of material layers are the same. A two-dimensional semiconductor simulation package, Atlas, was employed to analyze the energy-band

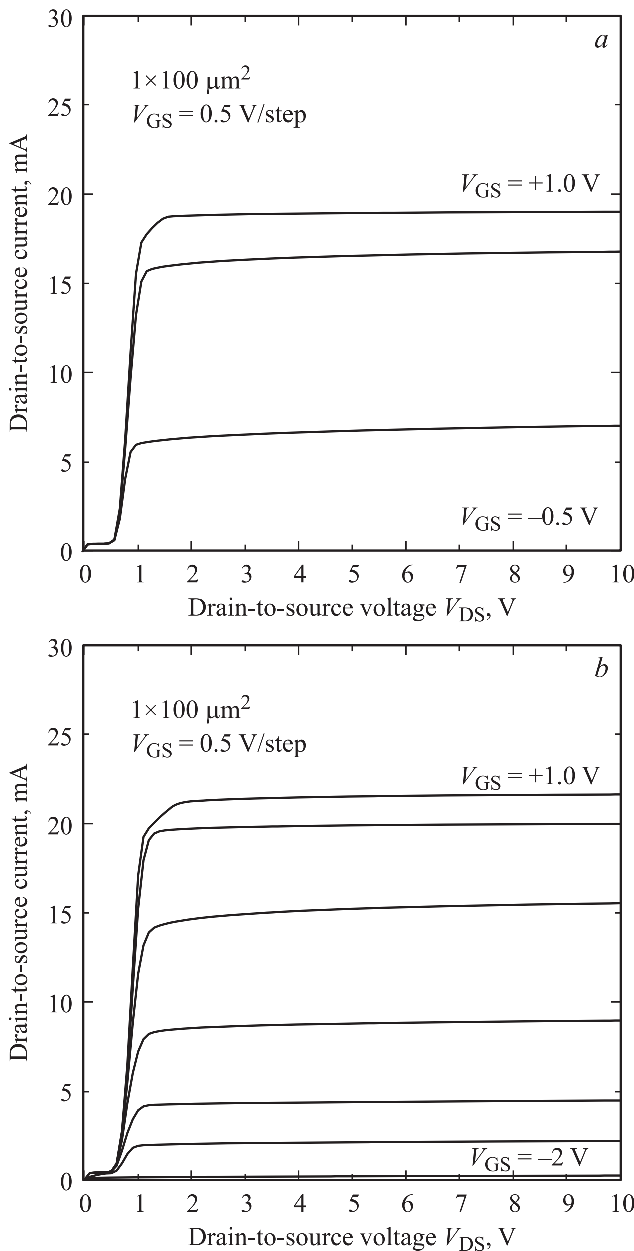

Figure 4. Common-source current–voltage characteristics of (*a*) device A and (*b*) device B.

diagrams, carrier distributions, DC, and high-frequency performance [10]. The analysis takes into account the Poisson equation, continuity equation of electrons and holes, Shockley–Read–Hall (SRH) recombination, Auger recombination, and Boltzmann statistics, simultaneously. Fig. 1, *a* and *b* show the schematic cross section of the devices A and B, respectively. The gate dimension and drain–to–source spacer were $100\,\mu m^2$ and $3\,\mu m$, respectively.

3. Results and discussion

The energy band diagrams at equilibrium of the devices A and B are illustrated in Fig. 2, *a* and *b*, respectively. The large conductance band discontinuity at InGaP/GaAs heterojunction and the undoped InGaP gate layer with large energy gap could provide a large gate potential barrier height ϕ preventing the injection of carriers into gate electrode from the channel and increases the gate forward bias. In the device A, the upper δ-doped supplied layer was placed below the InGaP gate layer and 2DEG is formed at the front of GaAs channel to contribute the conducting current, while it is formed at the bottom of the GaAs channel in device B with lower δ-doped supplied layer. As seen in the figures, the gate potential barrier height of 1.374 V in device A is less than that of 1.416 V in device B because the upper

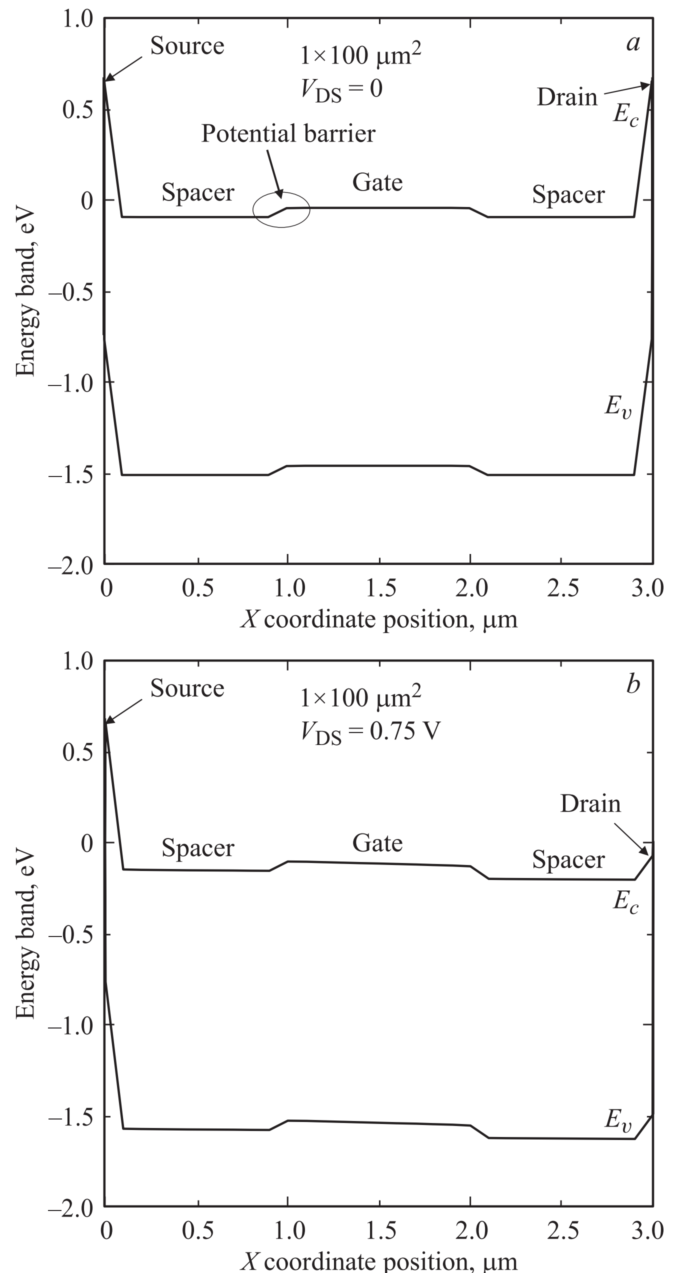

Figure 5. Energy band diagrams of device A along the 2DEG channel from source to drain region (*a*) at equilibrium and (*b*) $V_{DS} = 0.75\,V$.

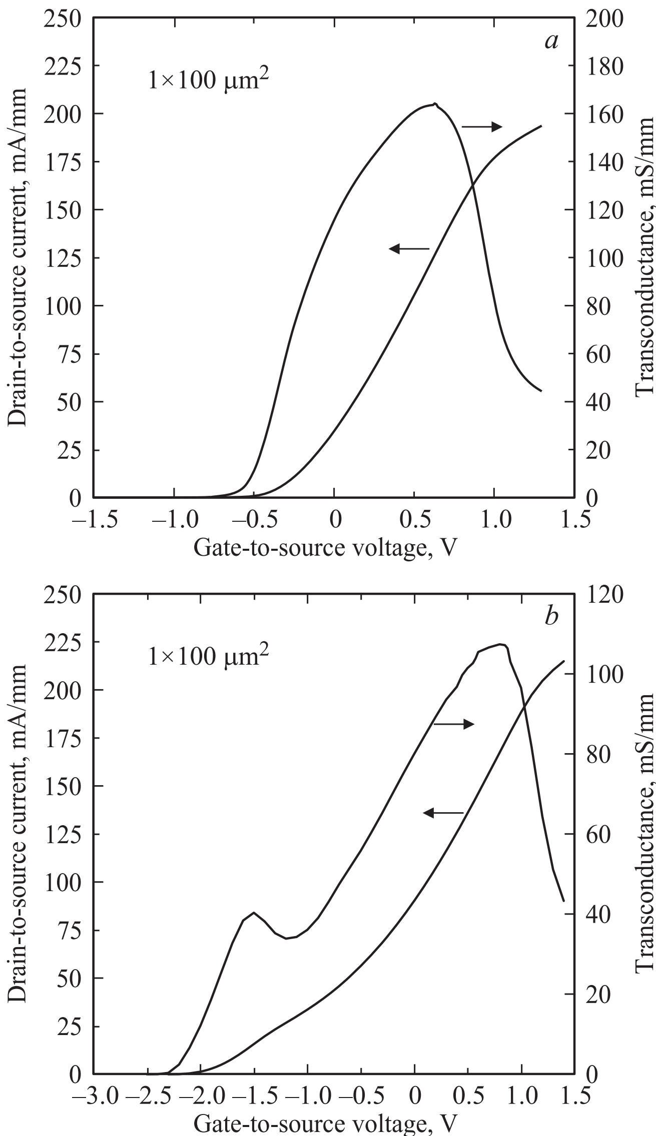

Figure 6. Drain current density and transconductance versus gate voltages at $V_{DS} = +6$ V for (a) device A and (b) device B.

δ-doped supplied layer and the 2DEG in channel could be depleted easily by metal–semiconductor gate Schottky contact. Fig. 3, a and b show the electronic distributions at equilibrium of the devices A and B, respectively. The peak concentration of channel is $1.401 \cdot 10^{19}\,\mathrm{cm}^{-2}$ in the devices B, which is greater than that of $2.748 \cdot 10^{18}\,\mathrm{cm}^{-2}$ in the device A. Because the position of delta-doped supplied layer in device B is far from gate electrode, the effect of gate depletion versus gate bias is slight and the device shows a higher 2DEG concentration as compared with the device A. Fig. 4, a and b depict the common-source current–voltage ($I-V$) characteristics of the devices A and B, respectively. The gate voltage is biased by a voltage step of 0.5 V. The device B exhibits broad gate voltage swing than the device A. A maximum drain current of 18.95 (21.59) mA at gate-to-source voltage of $+1$ V is observed for the device A (device B). It is worthy to note that an apparent knee effect in $I-V$ curves is observed at low drain-to-source voltage in the two devices. This phenomenon is described in the following. For the case of device A, the energy band diagrams along the 2DEG channel from source to drain region at equilibrium and $V_{DS} = 0.75$ V are illustrated in Fig. 5, a and b, respectively. Clearly, there is a higher 2DEG concentration under the two spacer region than that under the gate region because the gate depletion only occurs below the gate metal. Thus, the carrier transportation along the 2DEG channel will face a potential barrier below the gate metal at small drain-to-source voltage, as seen in Fig. 5, a. Nevertheless, at somewhat drain-to-source voltage, i. e., $V_{DS} = 0.75$ V, the potential barrier is lower and electrons can easily transport along the 2DEG channel from

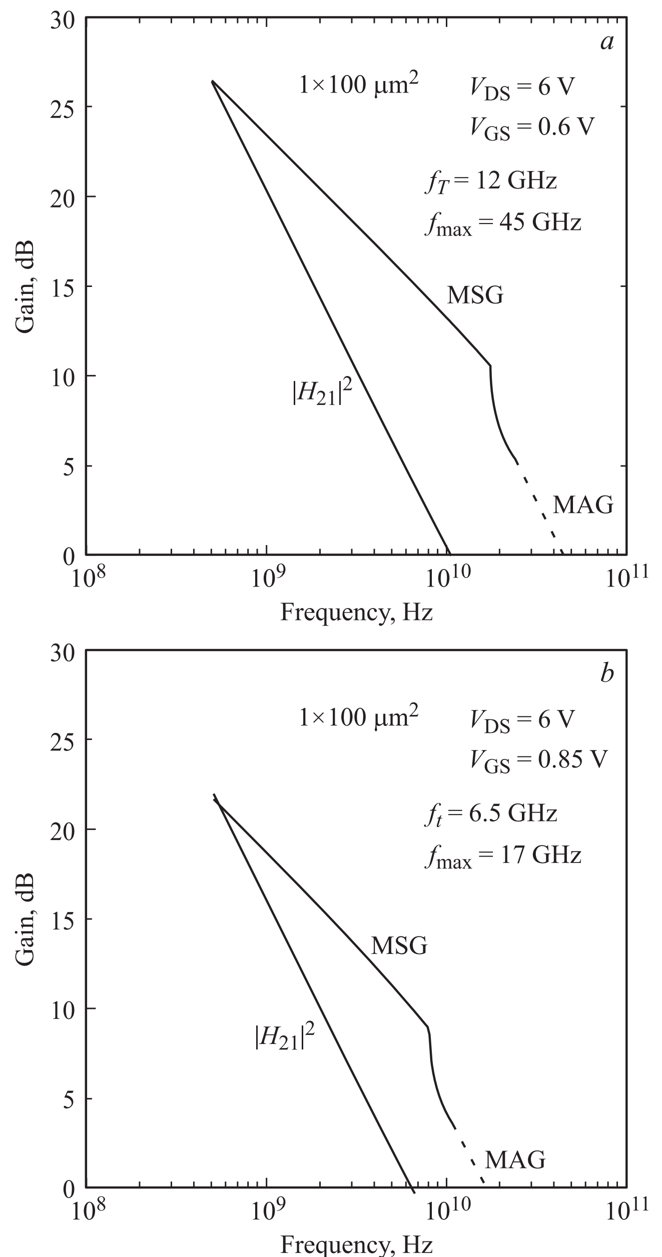

Figure 7. Microwave characteristics of (a) device A and (b) device B.

source to drain, as seen in Fig. 5, *b*. In this condition, the drain current will rapidly increase.

Fig. 6, *a* and *b* shows the drain current density and transconductance versus the gate voltage when the drain-to-source voltage is fixed at $+6$ V for the devices A and B, respectively. An extrinsic transconductance of 164.3 (107.4) mS/mm and a maximum drain current density of 193.7 (214.9) mA are observed in the device A (device B). The maximum current density of device B is greater than the device A, which can be attributed from the higher gate barrier height and better confinement effect for carriers in channel. However, the maximum transconductance value of device B is lower than the device A attributed that the position of 2DEG in the GaAs channel is far from the gate. In addition, the threshold voltage of -0.48 V (-2.04 V) as the drain current is defined at 1 mA/mm are depicted for the device A (device B). The device B can be operated to more negative gate bias due to the higher 2DEG concentration in channel.

The microwave characteristics of the devices A and B are illustrated in Fig. 7, *a* and *b*, respectively. The unity current gain cut-off frequency f_t is of 12 (6.5) GHz and the maximum oscillation frequency $f_{\max}$ is of 45 (17) GHz in the device A (device B). The microwave performance of device B is inferior than the device A due to the lower transconductance value and larger parasitic capacitance. These performance could be improved by reducing the gate length.

4. Conclusion

In summary, the characteristic difference of InGaP/GaAs HEMTs with upper and lower δ-doped supplied layers have been demonstrated. For comparison, the device with lower δ-doped layer exhibits higher gate potential height, higher drain current, and broader gate voltage swing, though it has lower transconductance and inferior high-frequency characteristics. Furthermore, a knee effect in $I-V$ curves is observed at low drain-to-source voltage. This could be attributed that electrons transportation along the 2DEG channel faces a potential barrier below the gate metal region at low drain-to-source voltage. Consequently, the comparison of the proposed devices provides a good potential for device design in signal amplifier and circuit applications.

Acknowledgment: This work is supported by the National Science Council of the Republic of China under Contract No. NSC 99–2221-E-017-018 and NSC 100-2221-E-017-001.

References

[1] R.H. Caverly, K.J. Heissler. IEEE Trans. Microwave Theory and Techniques, **48**, 98 (2000).
[2] Y.S. Lin, B.Y. Chen. J. Electrochem. Soc., **154**, H951 (2007).
[3] Y.S. Lee, M.W. Lee, Y.H. Jeong. IEEE Microwave and Wireless Components Lett., **18**, 55 (2008).
[4] F. Ren, R. Kopf, J. Kuo, J. Lothian, J. Lee, S. Pearton, R. Shul, C. Constantine, D. Johnson. Sol. St. Electron., **42**, 749 (1998).
[5] S.J. Yu, W.C. Hsu, Y.J. Chen, C.L. Wu, Sol. St. Electron., **50**, 291 (2006).
[6] J.H. Tsai, C.M. Li, W.C. Liu, D.F. Guo, S.Y. Chiu, W.S. Lour. Electron. Lett., **43**, 732 (2007).
[7] L.Y. Chen, S.Y. Cheng, T.P. Chen, K.Y. Chu, T.H. Tsai, Y.C. Liu, X.D. Liao, W.C. Liu. IEEE Trans. Electron. Dev., **55**, 3310 (2008).
[8] M.K. Tsai, S.W. Tan, Y.W. Wu, W.S. Lour, Y.J. Yang. Semicond. Sci. Technol. **17**, 156 (2002).
[9] W.C. Liu, W.L. Chang, W.S. Lour, K.H. Yu, K.W. Lin, C.C. Cheng, S.Y. Cheng. IEEE Trans. Electron. Dev., **48**, 1290 (2001).
[10] SILVACO 2000 Atals User's Manual Editor I, (SILVACO Int. Santa Clara, CA, USA).

Редактор Т.А. Полянская